University of Reading

Designing wearable sensing platforms for healthcare in a residential environment

Article

Published Version

Creative Commons: Attribution 3.0 (CC-BY)

Open Access

Fafoutis, X., Vafeas, A., Janko, B., Sherratt, R. S. ORCID: https://orcid.org/0000-0001-7899-4445, Pope, J., Elsts, A., Mellios, E., Hilton, G., Oikonomou, G., Piechocki, R. and Craddock, I. (2017) Designing wearable sensing platforms for healthcare in a residential environment. EAI Endorsed Transactions on Pervasive Health and Technology, 3 (12). 153063. ISSN 2411-7145 doi: 10.4108/eai.7-9-2017.153063 Available at https://centaur.reading.ac.uk/72370/

It is advisable to refer to the publisher's version if you intend to cite from the work. See Guidance on citing.
Published version at: http://eudl.eu/doi/10.4108/eai.7-9-2017.153063
To link to this article DOI: http://dx.doi.org/10.4108/eai.7-9-2017.153063

Publisher: European Union Digital Library

All outputs in CentAUR are protected by Intellectual Property Rights law, including copyright law. Copyright and IPR is retained by the creators or other copyright holders. Terms and conditions for use of this material are defined in the End User Agreement.

www.reading.ac.uk/centaur

University of Reading

CentAUR

Central Archive at the University of Reading

Reading's research outputs online

EAI Endorsed Transactions
on Pervasive Health and Technology
Research Article EAI.EU

Designing Wearable Sensing Platforms for Healthcare in a Residential Environment

Xenofon Fafoutis[1,*], Antonis Vafeas[1], Balazs Janko[2], R. Simon Sherratt[2], James Pope[1], Atis Elsts[1], Evangelos Mellios[1], Geoffrey Hilton[1], George Oikonomou[1], Robert Piechocki[1] and Ian Craddock[1]

[1]Department of Electrical and Electronic Engineering, University of Bristol, Woodland Road, Bristol, BS8 1UB, UK
[2]Department of Biomedical Engineering, University of Reading, Whiteknights, Reading, RG6 6AY, UK

Abstract

Wearable technologies are valuable tools that can encourage people to monitor their own well-being and facilitate timely health interventions. In this paper, we present SPW-2; a low-profile versatile wearable sensor that employs two ultra low power accelerometers and an optional gyroscope. Designed for minimum maintenance and a long-term operation outside the laboratory, SPW-2 is able to offer a battery lifetime of multiple months. Measurements on its wireless performance in a real residential environment with thick brick walls, demonstrate that SPW-2 can fully cover a room and - in most cases - the adjacent room, as well.

Received on 31 August 2016; accepted on 05 September 2017; published on 07 September 2017

Keywords: Wearable Technology, Bluetooth Low Energy, IEEE 802.15.4, Internet of Things, eHealth, Digital Health

Copyright © 2017 X. Fafoutis *et al.*, licensed to EAI. This is an open access article distributed under the terms of the Creative Commons Attribution license (http://creativecommons.org/licenses/by/3.0/), which permits unlimited use, distribution and reproduction in any medium so long as the original work is properly cited.

doi:10.4108/eai.7-9-2017.153063

1. Introduction

The increasing trends in elderly populations [8] and the continuous rise of chronic medical conditions, such as depression and diabetes, push the limits of national health systems [7]. Wearable technologies [5] and Ambient Assisted Living (AAL) infrastructures are widely considered promising directions that could encourage people to monitor their own well-being and facilitate timely interventions.

In addition to health-oriented applications, long-term activity monitoring with wearable technologies is a tool that facilitates health-oriented research. Avon Longitudinal Study of Parents and Children (ALSPAC) is a cohort study of children born in the county of Avon in England. During the first stage of the study in the early 90s, thousands of pregnant women were monitored. More recently, the study continues; monitoring the grandchildren of the originally monitored subjects [22] and the researchers adopt wearable technologies to replace diaries. SPHERE (a Sensor Platform for Healthcare in a Residential Environment) is an interdisciplinary research collaboration that aims to monitor volunteers in their own home environment [31]. Wearable sensors are used, among other sensing modalities, to monitor the everyday behaviour of the users [10].

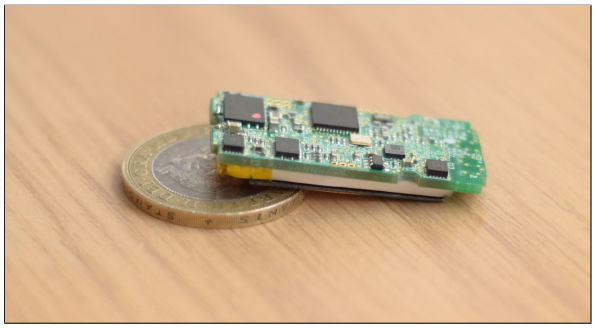

Figure 1. SPW-2: The Second SPHERE Wearable.

Long-term activity monitoring outside the laboratory, such as monitoring the activities of daily life in a residential environment, introduces important challenges that typically do not rise in controlled laboratory environments. The employed wearable devices need to be small, lightweight, comfortable and with

*Corresponding author. Email: xenofon.fafoutis@bristol.ac.uk

minimum maintenance requirements. Contrary to fashionable wearable gadgets that implement fitness application, wearable devices that are aimed for healthcare applications cannot depend on the user for regular maintenance, such as recharging or replacing the battery. As an example, consider patients suffering from mental conditions. In such situations, the user is not in a position to maintain the technology that supports them. In addition, in health-oriented research studies outside the laboratory, long battery lifetime increases the reliability of data collection, as the problem of data loss, due to improper maintenance of the technologies used, is mitigated.

With the aforementioned requirements as the primary goal, this paper focuses on system-level challenges of designing wearable sensors for healthcare in a residential environment. In this context, we present SPW-2 (the Second SPHERE Wearable), shown in Fig. 1. SPW-2 extends our previous work [9], building on the experience gained by using SPW-1 (the First SPHERE Wearable) in health-oriented studies in real environments. The contribution of this work is twofold. Beyond offering a tool to the pervasive health research community, we provide insight to researchers and engineers who are developing similar systems. In particular, (i) we provide a thorough energy consumption study that is the basis of meaningful battery lifetime estimations for different sensor configurations; (ii) we demonstrate how various sensor configurations affect the lifetime of wearable devices; (iii) we quantify the performance of wireless battery charging; and (iv) we identify the value of a stable power supply with respect to the quality of the measurements. Moreover, we study SPW-2's wireless performance in the context of body-centric communications. The study includes measurements both in a controlled (*i.e.* anechoic chamber) and in a residential environment.

The remainder of the paper is organised as follows. Section 2 summarises the related work. Section 3 presents the system design of our wearable sensors. Section 4 evaluates SPW-2's performance and compares it to its predecessor. Lastly, Section 5 concludes the paper.

2. Related Work

In recent years fashionable gadgets, such as Fitbit, Jawbone UP and Nike+ Fuelband SE, have appeared in the consumer electronics market [17]. Such fitness devices demonstrate the rise of a trend towards self-monitoring, as well as the willingness of users to wear them. These commercial gadgets are of limited use for research or medical applications due to limited access to the raw data, their lack of interoperability with other healthcare systems and their limited expandability to new sensor technologies. Furthermore, their need for regular recharging (typical battery lifetime of less than a week) hinders their suitability for target groups that are uncomfortable with or physically unable of managing modern technologies.

The research community has also used several wearable devices for activity monitoring, a few of which are briefly reviewed in this paper. We refer the reader to [5] for an exhaustive survey on smart wearable technologies. Verity [30] is an AAL platform that is using a wearable device equipped with an accelerometer and a piezo-resistive sensor for fall detection and heart rate monitoring. In [13], the authors propose an AAL platform based on a waist-worn accelerometer that is able to identify basic activities, such as sitting, walking, running and jumping. Similarly, [32] and [6] perform identification of basic activities using multiple on-body accelerometers and gyroscopes. These platforms use off-the-shelf hardware and do not focus on their power consumption, resulting to wearable devices that require regular recharging. Other works present low power hardware that target various body sensing applications by incorporating different types of sensors, such as bio-impedance sensors [18], microphones [21] and inertial sensors [15].

On a different perspective, related work on Wireless Body Area Networks (WBANs) typically focuses on the networking aspects of body sensor networks [28].

3. System Design

Wearable sensors can be arguably considered as the most resource-constrained things in the IoT, as they must be sufficiently small and lightweight to be comfortably worn by people. These physical requirements introduce several challenges in the system design. Their batteries, for instance, are of much smaller capacity compared to typical wireless sensor nodes. Their wireless performance is also constrained by their small form factor, which neither allows the use of antennas of high efficiency, nor provides the necessary space for sufficient isolation between the antenna and the other electronic components. In addition, wearable sensors are mobile - thus, with high dynamics in the wireless network - and the wireless signal is frequently shadowed by the body of the user. The application of wearable sensors for long-term monitoring for healthcare in a residential environment makes matters worse. Different to commercial fitness-oriented wearable platforms, which depend on the user for regular maintenance (*i.e.* recharging the battery), wearable sensors designed for residential healthcare, are targeted to groups of the population that are not necessarily comfortable with modern technology or capable of maintaining it.

Targeting the aforementioned system specifications, the SPHERE wearable sensors are designed with the

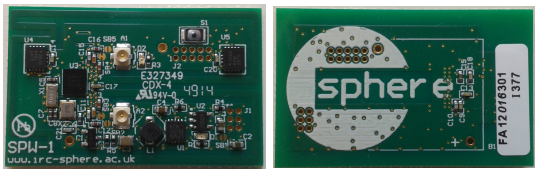

Figure 2. SPW-1: Top view (left) and bottom view (right) of the circuit board.

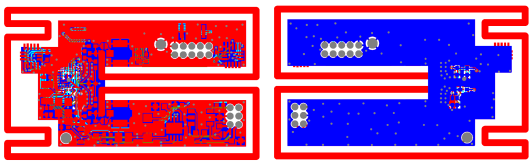

Figure 3. SPW-1: Top copper layer (left) and bottom copper layer (right) of the circuit board. The differentially-fed loop antenna is printed around the other components.

wrist as the target body position. A wrist-mounted device is widely considered as the most socially-acceptable and least invasive choice to the subject's everyday routine, as people of both sexes often wear wrist-worn gadgets, such as watches and bracelets. Alternative body positions, such as the chest or the waist, can be realised via an appropriate enclosure, but hold the risk of being removed by the subject and compromising the effectiveness of the system. Social studies [33][3] have shown the importance of wearable devices being comfortable and not intrusive to the daily life activities. In [19], the authors assess various body positions and present comparison results in which the wrist ranks high in all the considered activities in terms of classification accuracy.

Our previous work is focused on SPW-1 [9], the first wearable platform of SPHERE, which is presented in Section 3.1. Section 3.2 extends our previous work, introducing the second generation of the SPHERE wearable platform, named SPW-2.

3.1. SPW-1: The First SPHERE Wearable

Fig. 2 shows the printed circuit board (PCB) of SPW-1, with dimensions of $24 \times 39 \times 3.8$ mm. The primary component is a nRF51822 system-on-chip (SoC) which incorporates an ARM Cortex M0 processor, 32KB of RAM, 256KB of non-volatile flash memory, and a Bluetooth Low Energy (BLE) radio [4]. Two ADXL362 accelerometers are interfaced, over SPI (Serial Peripheral Interface), to the nRF51822. The ADXL362 is a micro-power triaxial digital accelerometer that has 12-bit resolution (8-bit formatted data is also available for more efficient single-byte transfers), a maximum sampling frequency of 400 Hz, and supports measurement ranges of ±2g, ±4g, ±8g. It also employs a 512-sample FIFO buffer (First In First Out). The incorporation of two accelerometers, at a distance of 30 mm, provides a low power alternative to a gyroscope. Indeed, differential measurements from multiple accelerometers can be used to derive the angular acceleration [25][29]. The accelerometers are powered by the SoC through its GPIO (General Purpose Input Output) pins and hence is able to power them on and off individually. Therefore, the use of the second accelerometer is optional. The ADXL362 also provides two interrupt pins (INT1 and INT2) that can be used either to generate interrupts on events, or to generate events based on external triggers. The two INT1 pins of the accelerometers are connected to GPIO pins of nRF51822 with the purpose of generating interrupts that wake up the SoC. The two INT2 pins are connected, over the same bus, to a GPIO of the SoC as an input. Using INT2, the SoC generates a square wave signal that synchronises the accelerometers by triggering the measurements. The use of the interrupts is also optional.

Regarding powering options, SPW-1 is compatible with various sources. Ultra low power consumption is partially achieved by using the SoC in low power mode, *i.e.* at 1.8V. The system employs the LTC3388 DCDC (Direct Current to Direct Current) converter that efficiently converts any voltage source from 2.7V to 6V, to the required 1.8V. Thus, the converter supports multiple options, including 3V coin cell batteries (*e.g.* CR2032), 3.7V rechargeable Lithium-Polymer (Li-Po) batteries, and supercapacitors. Moreover, SPW-1 is energy harvesting ready, in the sense that any harvester that works at the appropriate voltage level, is compatible. The converter can be also bypassed, as the board provides direct access to the 1.8V trail. SPW-1 also employs an MCP73831, a 500 mA linear charge management controller with 4.2V output that is compatible with single cell 3.7V Li-Po batteries. The battery charger is, by default, isolated from the remaining of the circuit and can be optionally connected.

With regard to input and output interfaces, SPW-1 employs one button and two LEDs (Light Emitting Diodes). The button and one of the LEDs are controlled by the SoC and, thus, are available to the application. The other LED is connected to the battery charger indicating when the battery is charging. Moreover, external sensors can be connected to SPW-1, using 7 available GPIOs (all support digital inputs; 2 of them also support analogue inputs). The INT2 line of the accelerometers is also externally available, so that external sensors can be synchronised to the embedded accelerometers.

Energy awareness is also considered in the design. With a potential divider, the high voltage of the source is appropriately conditioned to the requirements of the SoC's analogue-to-digital converter (ADC). When a battery (*e.g.* CR2032) is used, this feature can be

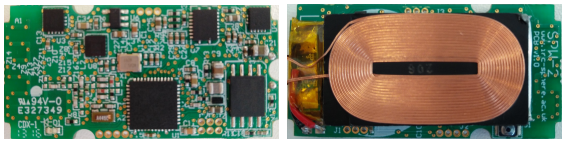

Figure 4. SPW-2: Top view (left) and bottom view (right) of the circuit board.

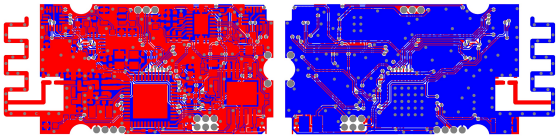

Figure 5. SPW-2: Top copper layer (left) and bottom copper layer (right) of the circuit board. SPW-2 employs a meandered inverted-F antenna.

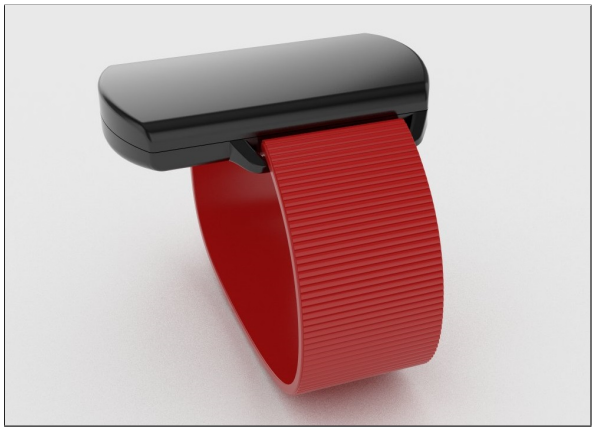

Figure 6. The enclosure of SPW-2.

used to issue low-battery warnings. In case of energy harvesting, energy-awareness allows the system to adapt to the available ambient energy.

As far as wireless is concerned, SPW-1 employs a meandered loop antenna printed on the FR4 substrate, matched to the differential RF output of the nRF51822 (shown in Fig. 3). The loop antenna was measured to have an efficiency of about 60% (relative to a high-efficiency reference antenna) and a maximum directivity of 7 dBi (computed from the measured 3D radiation pattern). The antenna was measured in isolation in an anechoic chamber. Furthermore, SPW-1 supports external antennas by incorporating u.FL connectors. Using solder-bridges, the user can select either the embedded loop antenna or the external antennas. The radio of the nRF51822 supports 7 transmission power levels ranging from −20 dBm to 4 dBm.

SPW-1 has been extensively used by the participants of research studies, conducted by SPHERE [27] and ALSPAC [22] in free-living conditions. Moreover, it has been used in research on energy harvesting solutions for wearable sensors [11]. The extended use of SPW-1 in various research projects exposed some its the weaknesses. These include: (i) long-term participants highlighted that SPW-1 would be more comfortable if it were smaller and thinner; (ii) its internal flash memory is not sufficient to allow outdoors usage; (iii) more stable voltage regulation is required for noiseless acceleration sampling; and (iv) its voltage regulator is not efficient when used with a supercapacitor, due to its high minimum input voltage (2.7V). In the next section, we build on this experience, introducing the second generation of the SPHERE wearable, SPW-2.

3.2. SPW-2: The Second SPHERE Wearable

Fig. 4 shows the PCB of SPW-2, with dimensions of 20 × 41 × 3 mm. The primary component is a CC2650 SoC which incorporates an ARM Cortex M3 processor, 30KB of RAM, 128KB of non-volatile flash memory, and a 2.4 GHz radio. The CC2650 offers more energy-efficient wireless connectivity, making SPW-2 more energy-efficient than its predecessor. In addition, CC2650 is more versatile as it is the first off-the-shelf radio that supports both BLE and IEEE 802.15.4 [1], the physical and link layer of 6LoWPAN, Zigbee [34] and Thread [24]. For a comprehensive comparison of BLE and IEEE 802.15.4, we refer the reader to the literature [20][12].

Similarly to SPW-1, SPW-2 employs two ADXL362 accelerometers. With SPW-1, we demonstrated the practical improvements in energy consumption of using a DCDC converter, instead of a linear voltage regulator [9]. Yet, the output voltage of the switching regulator has a 50 mV periodic fluctuation, which is introducing noise in the measurements of the ADXL362 accelerometers. SPW-2 mitigates this issue by incorporating two voltage regulators. A low-noise linear voltage regulator (TPS78318) provides the required 1.8V to the accelerometers, whilst a high-efficiency DCDC converter (TPS62746) powers the remaining board. Their combination improves the noise levels of the experiments at the cost of only a minor increase of the power consumption of the accelerometers (see Section 4).

Instead of a 5V input battery charger, SPW-2 employs the BQ51050B, a Qi-compliant [14] wireless power receiver and battery charger, that enables an inductive short-range wireless charging solution for 3.7V Li-Po batteries. The circuit is matched to a 7.5 μH low-profile (22 × 15 mm) Qi-compliant wireless power receiver coil (WE-WPCC). We opted for wireless charging and Li-Po batteries as the primary power source of SPW-2 for two reasons: it is a user-friendly means of replenishing the battery, and it enables the manufacturing of low-cost waterproof enclosures for the wearable sensor. In particular, SPW-2 is designed to fit a 100 mAh Li-Po (34 × 13 × 2.5 mm). This results to an overall thickness

Table 1. Summary of Features

Features	SPW-1	SPW-2
SoC	nRF51822	CC2650
BLE	Yes	Yes
IEEE 802.15.4	No	Yes
Processor	Cortex M0	Cortex M3
RAM	32KB	30KB
Internal Flash	256KB	128KB
Coin Cell Support	Yes	Yes
Li-Po Support	Yes	Yes
Battery Voltage	2.7 – 6 V	2.15 – 5.5 V
Battery Charger	Yes	Yes
Wireless Power (Qi)	No	Yes
Energy Awareness	Yes	Yes
Charging Awareness	No	Yes
Accelerometer	2	2
Gyroscope	No	Yes
External Flash	No	8MB
PCB Antenna	Yes	Yes
Max. Directivity	7 dBi	5.3 dBi
Max. Tx Power	+4 dBm	+5 dBm
External Antenna	Yes	No
LED	2	1
Button	1	1
GPIOs	7	5 (SPI)
Analogue GPIOs	2	3 (SPI)

of less than 7 mm, including the PCB, the battery and the wireless power receiver coil (see the enclosure of SPW-2 in Fig. 6).

In addition, SPW-2 incorporates a gyroscope (LSM6DS0). Gyroscopes require several orders of magnitude more power than the ADXL362 accelerometers. For this reason, the LSM6DS0 is powered from a GPIO, allowing it to be completely powered off when not needed. Furthermore, SPW-2 incorporates an 8 MB peripheral flash memory (MX25R6435F) that only consumes 200 nA in shutdown mode. Similarly to SPW-1, SPW-2 employs one button and one general purpose LED. Moreover, external sensors can be connected using 5 exposed GPIOs (all support digital inputs; 3 of them are shared with the SPI bus, but also support analogue input).

With regard to RF, SPW-2 employs a meandered inverted-F antenna printed on the FR4 substrate, matched to the differential RF output of the CC2650 (shown in Fig. 5). The antenna has a maximum directivity of 5.3 dBi. It should also be noted that CC2650 allows a higher transmission power of +5 dBm compared to the nRF51822 used by SPW-1.

Table 1 compares SPW-2 to SPW-1, summarising their features.

4. Performance Evaluation

In comparison to the first generation of the SPHERE wearable, SPW-2 has a smaller form factor, offering several additional features including wireless charging, a gyroscope, additional flash memory, and support for IEEE 802.15.4 (as summarised in Table 1). In this section, we evaluate the performance of SPW-2, in terms of energy consumption (providing realistic battery lifetime estimations), wireless coverage (using measurements in both an anechoic chamber and a residential environment), and its noise levels. Its performance is benchmarked against its predecessor, SPW-1, which was benchmarked against an off-the-shelf board in our previous work [9]. Moreover, we evaluate the performance of the wireless charger.

4.1. Power Profile and Battery Lifetime Estimations

In this section, we compare the energy consumption of SPW-1 and SPW-2, providing realistic estimations on their battery life. For both devices, we calculate the power profile by measuring the current through a 10 Ω series resistor on the positive side of the power source, as in [10]. Idle currents are measured with a digital multimeter. The supply voltage is 3.7V, that is the nominal voltage of Li-Po batteries.

SPW-1 yields a constant idle power consumption of 8.4 μW, which includes the idle consumption of the nRF51822 in sleep mode with the low frequency oscillator active, the idle consumption of the accelerometers deactivated, and the quiescent consumption of all the remaining components. Each accelerometer adds an extra constant power consumption of approximately 3 μW when active. SPW-2 employs several more components that are directly powered by the battery, including the external flash memory, the Qi wireless charger and the linear regulator. Because of the idle consumption of those components, SPW-2 yields a slightly higher overall idle consumption of 8.6 μW. In addition, SPW-2 powers the accelerometers through a linear regulator that generates less noise at the cost of less efficient voltage regulation. As a result, each accelerometer adds an extra constant power consumption of approximately 3.3 μW when active. The result of this design choice on the noise levels is evaluated in Section 4.1. Overall, the several additional features of SPW-2 contribute to a slightly higher idle power consumption.

Next, we measure the energy required by the radio for transmitting data. In particular, we compare SPW-1 and SPW-2 in BLE mode that is the communication protocol that is supported by both. We measure the energy consumption of the transmission of a triple BLE advertisement (*i.e.* 3 packets of 39 bytes) at all different transmission power levels. An example of the power profile of SPW-2 when transmitting a triple BLE advertisement at 5 dBm is shown in Fig. 7. The energy

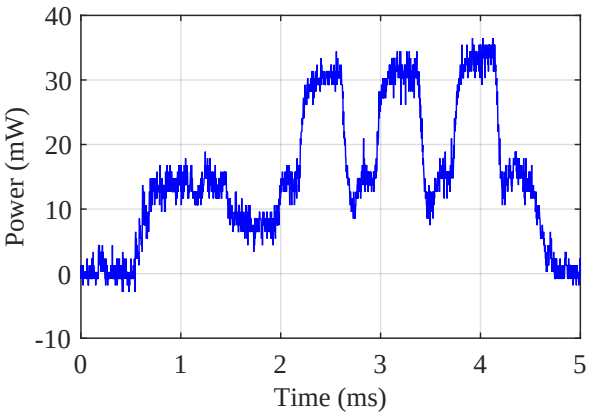

Figure 7. Power profile of SPW-2 when transmitting a triple BLE advertisement at 5 dBm.

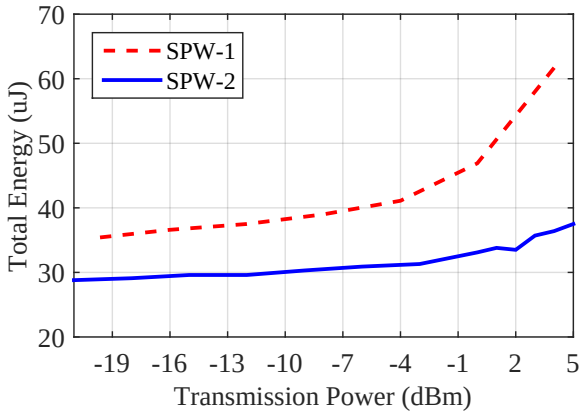

Figure 8. Energy consumption for the transmission of a triple BLE advertisement.

is then derived by calculating the integral of the power profile. Fig. 8 shows the total energy consumed for the transmission of a triple BLE advertisements at all supported transmission power levels for SPW-1 and SPW-2. SPW-2 performs significantly better, consuming approximately 40% less energy than SPW-1 at 4 dBm, and approximately 30% less energy at 0 dBm. In SPW-1, it can be observed that reducing the transmission power from the maximum level to −4 dBm is very beneficial for the battery lifetime, as it reduces the energy consumption for transmission by approximately 33%. In SPW-2 though, the transmission events are very energy-efficient. As a result, a similar reduction is less beneficial, as it reduces the energy consumption by approximately 17%.

We next evaluate the power required for using the processor. To measure the processing power, both platforms were programmed to perform some dummy processing cycles (integer multiplication and addition). The processing power of SPW-1 is 9.5 mW, whilst the processing power of SPW-2 is 8 mW. Transferring the data from the FIFO buffer of ADXL362 to the memory of the SoC takes approximately 0.2 ms (SPI clock at 4 MHz). Hence, transferring a single acceleration sample from the accelerometer to the SoC consumes approximately 1.9 μJ for SPW-1, and approximately 1.6 μJ for SPW-2.

Let us now combine the consumption measurements in an attempt to provide realistic battery lifetime estimations, based on an indicative scenario. Such estimations demonstrate how the lifetime of the battery scales with the configuration of different parameters, such as the number of sensors, the resolution, and the sampling frequency. In particular, we consider a scenario where the wearable device streams raw acceleration data using the undirected connectionless BLE advertisements (similarly to infrastructure presented in [10]). Although data reliability can be addressed at the receiver [26], this communication approach does not provide delivery guarantees and, thus, can be only applied to applications that can tolerate data loss or make use of specific missing data techniques [16]. We also assume the following. We assume that repetition coding on the three advertisements [10] is used to provide resilience to interference. We further assume the maximum BLE packet size of 39 bytes, which allows for 24 bytes of payload: 18 bytes used for acceleration data and 6 bytes are used for meta-data. This provides necessary space for either 4 triaxial samples of 12-bit resolution or 6 triaxial samples of 8-bit resolution. We also assume that the SPI bus between the sensors and the SoC is clocked at 4 MHz, the transmission power is set to its maximum level, and that the system is powered by a 100 mAh Li-Po battery (3.7V).

The battery lifetime estimations are based on the following equation:

$$T = \frac{E_{BAT}}{P_I + P_{XL} \times N + (E_{SPI} + E_{BLE}) \times f_s \times N}, \quad (1)$$

where E_{BAT} is the total energy of the battery; P_I is the idle power consumption; P_{XL} is the power consumption of a single accelerometer; E_{SPI} is the energy consumed for transferring a single acceleration sample over SPI from the accelerometer to the SoC; E_{BLE} is the energy consumed for the transmission of a single sample over BLE given by Fig. 8 and divided by the number of samples inside a packet; f_s is the sampling frequency; and N is the number of accelerometers.

Table 2 shows the battery lifetime estimations, in days, assuming different configuration scenarios. The frequency column represents the sampling frequency of the accelerometer(s) in Hz. Notice that the battery lifetime ranges from few days to years, depending on the configuration. Observe that at high sampling frequencies the energy consumption is dominated by frequent duty cycles. At low sampling frequencies,

Table 2. Battery Lifetime Approximations in Days

Platform	Freq.	1 Accel.		2 Accel.	
		8-bit	12-bit	8-bit	12-bit
SPW-1	0.1	990	951	742	699
	1	530	435	322	254
	10	93	67	48	34
	20	49	34	24	17
	50	20	14	10	7
	100	10	7	5	3
SPW-2	0.1	962	940	718	693
	1	623	539	396	330
	10	137	102	72	53
	20	73	53	37	27
	50	30	22	15	11
	100	15	11	7	5

instead, the idle consumption becomes increasingly more important. In [19], the authors use accelerometers with 8-bit resolution to perform activity classification. Experimenting with different sampling frequencies, the authors show that the performance of the classifier reaches a high level at approximately 10 Hz with only marginal improvement at higher frequencies. In this configuration, the battery lifetime of SPW-2 is approximated at 137 days. For comparison, SPW-1 yields a battery lifetime of approximately 93 days in the same configuration (an improvement of 47%). Indeed, SPW-2 yields higher battery lifetime than SPW-1 in most of the considered configuration scenarios. Due to its higher idle power though, this improvement decreases as the sampling frequency decreases. Eventually, at very low frequencies (see f = 0.1 Hz), SPW-1 performs better than SPW-2.

Let us now investigate how the use of the gyroscope affects the battery lifetime of SPW-2. With the gyroscope and one accelerometer activated, the battery lifetime estimations are based on the following equation:

$$T = \frac{E_{BAT}}{P_I + P_{XL} + P_{GY} + (E_{SPI} + E_{BLE}) \times f_s \times 2}, \quad (2)$$

where E_{BAT} is the total energy of the battery; P_I is the idle power consumption; P_{XL} is the power consumption of a single accelerometer; E_{SPI} is the energy consumed for transferring a single sample over SPI from the sensor to the SoC; E_{BLE} is the energy consumed for the transmission of a single sample over BLE given by Fig. 8 and divided by the number of samples inside a packet; and f_s is the sampling frequency. P_{GY} is the power consumption of the gyroscope, calculated from Table 10 of [23]. The transmission power is fixed to 5 dBm and the resolution of the samples is set to 12 bits.

Table 3. SPW-2: Battery Lifetime Approximations in Days

Frequency	Accel. Only	Accel. & Gyro.
10	102	3.2
20	53	2.4
50	22	2.1
100	11	1.8

Table 3 shows the battery lifetime estimations, in days, assuming different sampling frequencies for two scenarios: only one ADXL362 accelerometer is activated, and one ADXL362 accelerometer and the gyroscope are activated. It can be observed that the use of the gyroscope is responsible for a reduction of the battery lifetime of SPW-2 by one order of magnitude.

4.2. Charging Performance

SPW-2 employs a Qi-compatible wireless battery charger. To comply to the specifications of our target Li-Po battery (100 mAh), we have limited the charging current to 91 mA. Fig. 9 plots the charging the charging power of a full charging cycle when SPW-2 is in contact with a Qi-compatible off-the-shelf charging station. It can be observed that a full charging cycle takes approximately 80 minutes, whilst the charging rate decreases as the battery is reaching its full capacity. Fig. 10 shows the battery's state of charge as a function of time. The battery requires 63 minutes of charging to reach 90% of its full capacity.

In the next experiment, we explore the dependency of the maximum charging power to the distance of separation between the wearable and the charging station. The blue bars in Fig. 11 show the charging power at various distances when we do not limit the charging current. The horizontal line indicates the maximum charging power supported by our target battery (*i.e.* 0.37 W). It can be seen that the wireless charging system can support the maximum charging power of the battery for up to approximately 8 mm of separation between the wearable sensor and the charging station. For reference, when SPW-2 is inside its enclosure, shown in Fig. 6, its separation to charging station is 2 mm, including the strap.

4.3. Noise Levels

The offset of the acceleration measurements produced by the ADXL362 depends on its supply voltage. Therefore, the less noisy is voltage regulator, the less noisy are the data produced. SPW-1 powers the accelerometers through a DCDC high-efficiency voltage regulator, which is responsible for a 50 mV fluctuation on the power supply of the accelerometers. SPW-2 powers the accelerometers through a less efficient, yet less noisy linear regulator. In Section 4.1, we showed

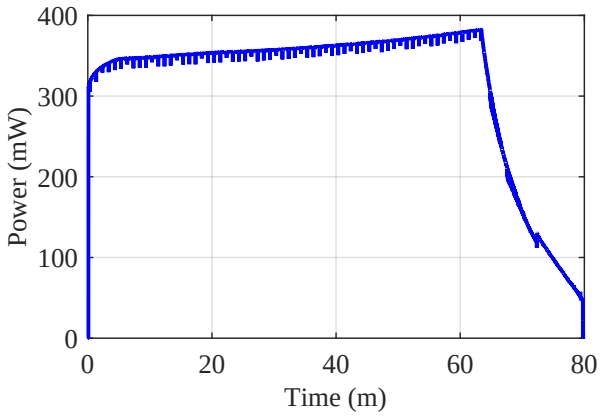

Figure 9. Charging power of a full charging cycle.

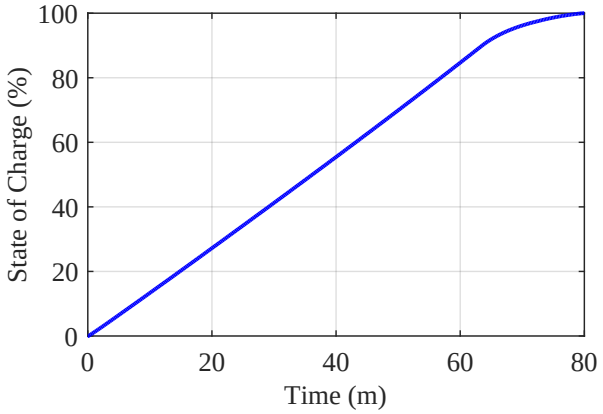

Figure 10. State of charge as a percentage of the battery capacity over the charging time.

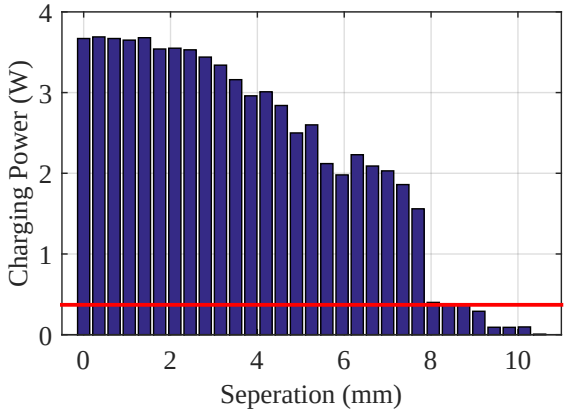

Figure 11. Charging power for various separation between the SPW-2 and the charging coil. The horizontal line indicates the maximum charging power supported by the employed battery.

how this approach affects the idle power of SPW-2. In this section, we quantify the benefits of this approach on the noise levels.

To this end, we let SPW-1 and SPW-2 immobile for 10 minutes, whilst collecting the acceleration measurements that they produce. Fig. 12 plots the histograms of the difference of each measurement from the mean value for each axis (SPW-1 is shown on top and SPW-2 is shown below). The standard deviation of the samples for SPW-1 are: 6 mg for the x-axis, 7.2 mg for the y-axis, and 6.9 mg for the z-axis. In contrast, the standard deviation of the samples for SPW-2 are: 4.6 mg for the x-axis, 5.1 mg for the y-axis, and 5.7 mg for the z-axis. The results demonstrate a substantial improvement in the noise levels.

4.4. Wireless Performance

In comparison to SPW-1, the 2.4 GHz antenna of SPW-2 has a smaller form factor; yet, it is better isolated from the other components. The former has a negative effect on its wireless performance, whereas the latter has a positive effect. In this section, we evaluate SPW-2's wireless performance. First, we benchmark SPW-2 against SPW-1 in an anechoic chamber, *i.e.* a controlled interference-free environment that eliminates the multipath components of the wireless signal. The experiments are constructed as follows. In one side of the room, we place the wearable sensor (SPW-1 and SPW-2). At the other side of the room, at a distance of 4.4 m, we place a receiver unit with two orthogonally polarised dipole antennas. The receiver unit is set in BLE scanner mode, in which it operates as a receiver, hopping among channels 37, 38, and 39, and logs the RSSI of all the received packets. In both experiments, the position of the receiver was fixed while two motors rotated the wearable device through all angles in 3D space.

Fig. 13 plots the CDF (cumulative distributed function) of the RSSI of all the packets received for SPW-1 and SPW-2. It can be observed that both wearable sensors yield an equal 40-th percentile. This indicates that they have identical wireless performance in the worst case scenarios. In better links though, SPW-2 demonstrates a marginally better performance - its 80-th percentile is approximately 1 dB higher.

We, next, evaluate the wireless performance of SPW-2 in a typical residential environment in the city of Bristol, UK. In each one of two adjacent rooms, we deployed a receiver unit identical to the ones used in the previous experiment, as shown in Fig. 14. SPW-2 was mounted on the wrist of a human, who was performing random walks and random activities within the room for approximately 30 minutes (room size: 3×3 m). Thus, the measurements capture the effect of body shadowing and multipath propagation in a wide variety of situations. Fig. 15 shows the CDF of the RSSI of all the received packets, as measured from the receivers located in the same room and the adjacent

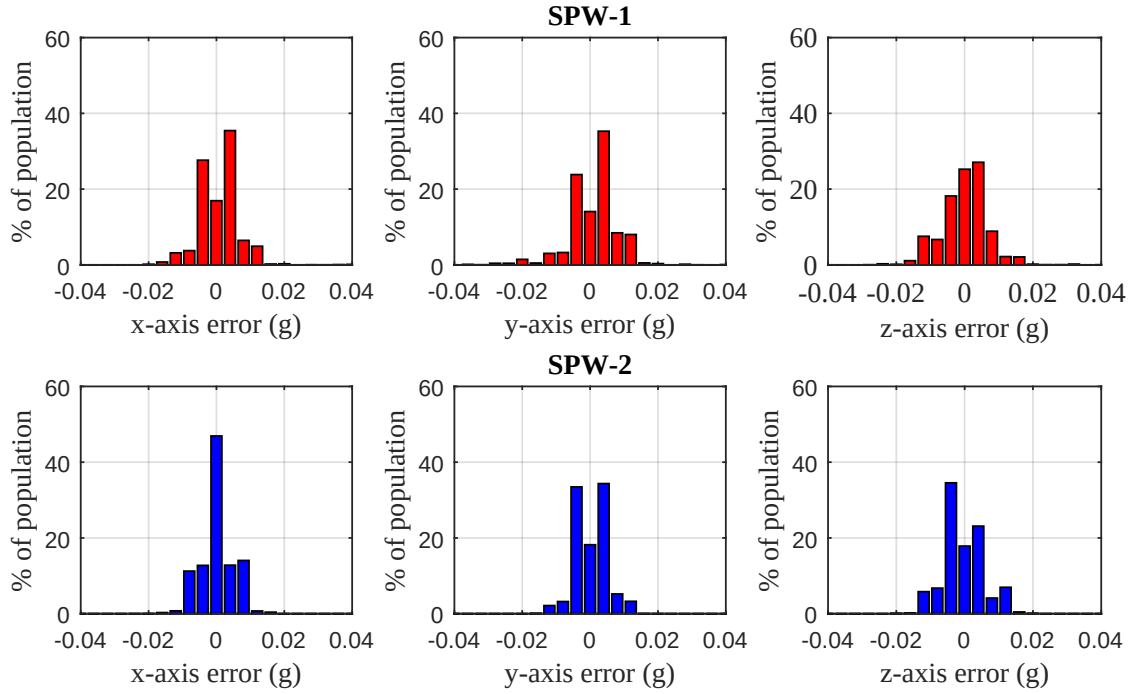

Figure 12. Noise levels of SPW-1 and SPW-2.

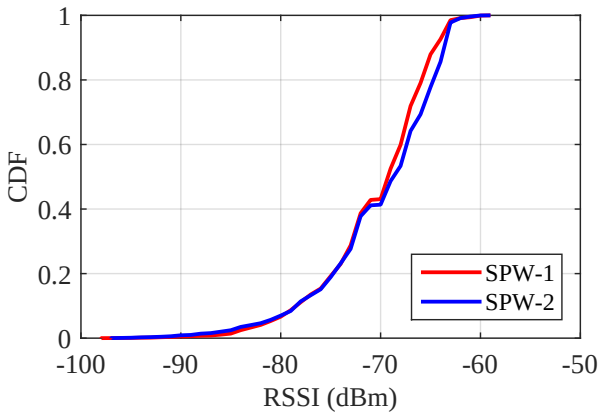

Figure 13. Comparison of the wireless performance of SPW-1 and SPW-2 in the anechoic chamber.

room respectively. At the maximum transmission power setting, observe that in the case of the same room, the RSSI ranges from −90 dBm to −39 dBm, whilst the median is at −62 dBm. In the adjacent room, the RSSI ranges from −100 dBm to −55 dBm, whilst the median is at −76 dBm. Our previous measurements indicate that the packet error probability threshold of 1% is at −93 dBm when CC2650 is in BLE mode [12]. As a result, SPW-2 can fully cover a single room with less than 1% probability of error, as well as most of the cases of the adjacent room. It is approximated that one BLE receiver per two rooms is required for full-house coverage. A more comprehensive study on providing full-house wireless coverage for wearable sensors in a residential environment like the SPHERE house can be found in [2].

5. Conclusion

This work is focused on the system-level challenges of designing wearable sensors for pervasive health, presenting SPW-2, our wearable activity sensing platform. This paper extends our previous work on SPW-1 [9], building upon the experience of using SPW-1 in experiments outside of the laboratory.

SPW-2 is based on two accelerometers for activity sensing and either BLE or IEEE 802.15.4 for wireless communication. Aimed for long-term activity monitoring, SPW-2 is a lightweight wearable sensor that decreases the dependency on the user for maintenance. In typical residential healthcare scenario, such as the sensing system presented in [10], SPW-2 can yield a battery lifetime of several months. Indeed, as shown in this paper, the battery lifetime of wearable sensors depends a lot on the configuration (resolution, sampling frequency) of their sensors, ranging from days to years. Indicatively, at a sampling frequency of 10 Hz and 8-bit resolution (a configuration used in [19]), the estimated battery lifetime of SPW-2 is 137 days, enabling long-term monitoring applications in scenarios that require low maintenance (*e.g.* monitoring

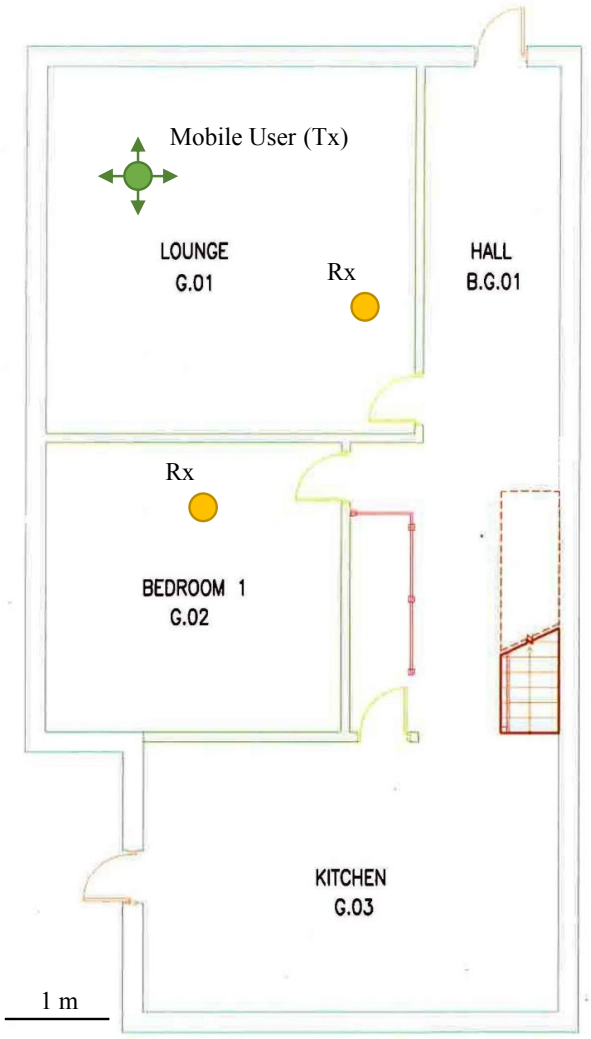

Figure 14. The floor plan of the SPHERE house. Two receiver units are deployed in the lounge and the bedroom. SPW-2 is mounted on the wrist of a user who is performing random walks and activities in the lounge.

patients that suffer from conditions that prevent them from regularly maintaining their wearable sensors).

With respect to its predecessor, SPW-2 offers a variety of new features that include: wireless charging, an optional gyroscope, an external flash memory, and support for IEEE 802.15.4 that makes it compatible with additional protocol stacks (*e.g.* Zigbee and Thread). In addition, SPW-2 is more energy-efficient, produces data of higher fidelity, and offers a similar wireless range despite its smaller form factor.

SPW-2 will be part of the SPHERE sensing platform [31] that will be deployed in the houses of 100 volunteers in the city of Bristol, UK, in 2017. In these deployments, each house resident will wear SPW-2 for a year, and the data will be published for further research in digital health.

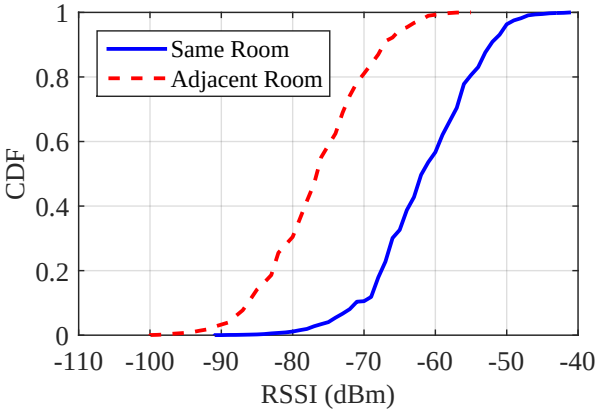

Figure 15. Wireless performance of SPW-2 in the a residential environment.

Acknowledgment

This work was performed under the SPHERE (a Sensor Platform for Healthcare in a Residential Environment) IRC funded by EPSRC, Grant EP/K031910/1. This work was supported in part by the EurValve Project (Personalised Decision Support for Heart Valve Disease), Project Number: H2020 PHC-30-2015 689617.

We would also like to thank Altium Ltd and Premier EDA Solutions Ltd for sponsoring Altium Designer licenses, and Simtek EMS Ltd for partially sponsoring and performing PCB and prototype production services.

References

[1] (2006) IEEE Standard for Information Technology-Telecommunications and Information Exchange Between Systems- Local and Metropolitan Area Networks- Specific Requirements Part 15.4: Wireless Medium Access Control (MAC) and Physical Layer (PHY) Specifications for Low-Rate Wireless Personal Area Networks (WPANs). doi:10.1109/ieeestd.2006.232110.

[2] Abdullah, M.W., Fafoutis, X., Mellios, E., Klemm, M. and Hilton, G. (2015) Investigation into Off-Body Links for Wrist Mounted Antennas in Bluetooth Systems. In *Proc. Loughborough Antennas and Propagation Conf. (LAPC)*.

[3] Bergmann, J. and McGregor, A. (2011) Body-worn sensor design: What do patients and clinicians want? *Ann. Biomedical Eng.* **39**(9).

[4] Bluetooth SIG (2010) Specification of the Bluetooth System - Covered Core Package version: 4.0.

[5] Chan, M., Estève, D., Fourniols, J.Y., Escriba, C. and Campo, E. (2012) Smart wearable systems: current status and future challenges. *Artif. Intell. Med.* **56**(3): 137–56. doi:10.1016/j.artmed.2012.09.003.

[6] Cheng, J., Chen, X. and Shen, M. (2013) A framework for daily activity monitoring and fall detection based on surface electromyography and accelerometer signals. *IEEE J. Biomedical and Health Informatics* **17**(1): 38–45.

[7] Cruz-Jentoft, A.J., Franco, A., Sommer, P., Baeyens, J.P., Jankowska, E., Maggi, A., Ponikowski, P. *et al.* (2009) Silver paper: the future of health promotion and preventive actions, basic research, and clinical aspects of age-related disease–a report of the European Summit on Age-Related Disease. *Aging Clin. Exp. Res.* **21**(6): 376–385.

[8] Department of Economic and Social Affairs - United Nations (2011) *World Population Ageing: 1950-2050*. Tech. rep.

[9] Fafoutis, X., Janko, B., Mellios, E., Hilton, G., Sherratt, R.S., Piechocki, R. and Craddock, I. (2016) SPW-1: A Low-Maintenance Wearable Activity Tracker for Residential Monitoring and Healthcare Applications. In *Proc. of the Int. Conf. on Wearables in Healthcare (HealthWear)*.

[10] Fafoutis, X., Tsimbalo, E., Mellios, E., Hilton, G., Piechocki, R. and Craddock, I. (2016) A residential maintenance-free long-term activity monitoring system for healthcare applications. *EURASIP Journal on Wireless Communications and Networking* **2016**(31). doi:10.1186/s13638-016-0534-3.

[11] Fafoutis, X., Clare, L., Grabham, N., Beeby, S., Stark, B., Piechocki, R. and Craddock, I. (2016) Energy Neutral Activity Monitoring: Wearables Powered by Smart Inductive Charging Surfaces? In *Proc. 13th IEEE International Conference on Sensing, Communication and Networking (SECON)* (IEEE).

[12] Fafoutis, X., Tsimbalo, E., Zhao, W., Chen, H., Mellios, E., Harwin, W., Piechocki, R. *et al.* (2016) BLE or IEEE 802.15.4: Which Home IoT Communication Solution is more Energy-Efficient? *EAI Transactions on Internet of Things* .

[13] Gupta, P. and Dallas, T. (2014) Feature Selection and Activity Recognition System Using a Single Triaxial Accelerometer. *IEEE Trans. Biomedical Engineering* **61**(6): 1780–1786.

[14] Hui, S. (2013) Planar Wireless Charging Technology for Portable Electronic Products and Qi. *Proceedings of the IEEE* **101**(6): 1290–1301. doi:10.1109/JPROC.2013.2246531.

[15] Kan, Y.C. and Chen, C.K. (2012) A Wearable Inertial Sensor Node for Body Motion Analysis. *IEEE Sens. J.* **12**(3): 651–657. doi:10.1109/JSEN.2011.2148708.

[16] Karadogan, S., Marchegiani, L., Hansen, L. and Larsen, J. (2011) How efficient is estimation with missing data? In *Proc. 2011 IEEE Int. Conf. on Acoustics, Speech and Signal Processing (ICASSP)* (IEEE): 2260–2263. doi:10.1109/ICASSP.2011.5946932.

[17] Kooiman, T.J.M., Dontje, M.L., Sprenger, S.R., Krijnen, W.P., van der Schans, C.P. and de Groot, M. (2015) Reliability and validity of ten consumer activity trackers. *BMC Sports Sci. Med. Rehabil.* **7**(1): 24. doi:10.1186/s13102-015-0018-5.

[18] Lee, S., Polito, S., Agell, C., Mitra, S., Firat Yazicioglu, R., Riistama, J., Habetha, J. *et al.* (2013) A Low-power and Compact-sized Wearable Bio-impedance Monitor with Wireless Connectivity. *J. Phys. Conf. Ser.* **434**(1): 012013. doi:10.1088/1742-6596/434/1/012013.

[19] Maurer, U., Smailagic, A., Siewiorek, D. and Deisher, M. (2006) Activity recognition and monitoring using multiple sensors on different body positions. In *Int. Workshop on Wearable and Implantable Body Sensor Networks (BSN)*.

[20] Mikhaylov, K., Plevritakis, N. and Tervonen, J. (2013) Performance Analysis and Comparison of Bluetooth Low Energy with IEEE 802.15.4 and SimpliciTI. *J. Sens. Actuator Networks* **2**(3): 589–613.

[21] Oletic, D., Arsenali, B. and Bilas, V. (2014) Low-power wearable respiratory sound sensing. *Sensors (Basel).* **14**(4): 6535–66. doi:10.3390/s140406535.

[22] Pearson, H. (2012) Children of the 90s: Coming of age. *Nature* **484**: 155–158.

[23] STMicroelectronics (2014) LSM6DS0 - iNEMO inertial module: 3D accelerometer and 3D gyroscope, Rev 3.

[24] Thread Group (2015) Thread Stack Fundamentals V2.

[25] Tsai, Y.L., Tu, T.T., Bae, H. and Chou, P. (2010) Ecoimu: A dual triaxial-accelerometer inertial measurement unit for wearable applications. In *Proc. Int. Conf. Body Sensor Networks (BSN)*: 207–212. doi:10.1109/BSN.2010.47.

[26] Tsimbalo, E., Fafoutis, X. and Piechocki, R. (2015) Fix it, don't bin it! - CRC error correction in Bluetooth Low Energy. In *Proc IEEE 2nd World Forum on Internet of Things (WF-IoT)*: 286–290. doi:10.1109/WF-IoT.2015.7389067.

[27] Twomey, N., Diethe, T., Kull, M., Song, H., Camplani, M., Hannuna, S., Fafoutis, X. *et al.* (2016) The SPHERE challenge: Activity recognition with multimodal sensor data. *arXiv preprint arXiv:1603.00797* .

[28] Ullah, S., Higgins, H., Braem, B., Latre, B., Blondia, C., Moerman, I., Saleem, S. *et al.* (2012) A Comprehensive Survey of Wireless Body Area Networks. *J. of Medical Systems* **36**(3): 1065–1094.

[29] Villeneuve, E., Harwin, W., Holderbaum, W., Sherratt, R.S. and White, R. (2016) Signal quality and compactness of a dual-accelerometer system for gyro-free human motion analysis. *IEEE Sensors Journal* **16**(16): 6261–6269. doi:10.1109/JSEN.2016.2582262.

[30] Winkley, J., Jiang, P. and Jiang, W. (2012) Verity: an ambient assisted living platform. *IEEE Trans. Consumer Electronics* **58**(2): 364–373.

[31] Woznowski, P., Fafoutis, X., Song, T., Hannuna, S., Camplani, M., Tao, L., Paiement, A. *et al.* (2015) A Multi-modal Sensor Infrastructure for Healthcare in a Residential Environment. In *Proc. Int. Conf. Communications (ICC) Workshops*.

[32] Zhang, Y., Markovic, S., Sapir, I., Wagenaar, R. and Little, T. (2011) Continuous functional activity monitoring based on wearable tri-axial accelerometer and gyroscope. In *Proc. 5th Int. Conf. Pervasive Computing Technologies for Healthcare (PervasiveHealth)*: 370–373.

[33] Ziefle, M. and Rocker, C. (2010) Acceptance of pervasive healthcare systems: A comparison of different implementation concepts. In *Proc. 4th Int. Conf. Pervasive Comput. Technologies for Healthcare (PervasiveHealth)*: 1–6.

[34] ZigBee Standards Organization (2008) ZigBee Specification: Document 053474r17.